参赛学生姓名：　刘奕成，陈允萱

中学：　北京市十一学校

省份：　北京市

国家/_地区：　中国

指导老师姓名：　董原辰

指导老师单位：　中国科学院化学研究所

指导老师姓名：　刘硕

指导老师单位：　北京市十一学校

论文题目：

Screening Allele-Specific siRNA for Single-Nucleotide-Mutated Type 3 Rickets

2026 S. T. Yau High School Science Award
仅用于2026丘成桐中学科学奖论文公示

论文题目： Screening Allele-Specific siRNA for Single-Nucleotide-Mutated Type 3 Rickets

作者： Yichen Liu, Yunxuan Chen, Shuo Liu, Yuanchen Dong,

论文摘要：

The single-nucleotide mutation of cytochrome P450 3A4 was recently identified as the cause of vitamin D-dependent rickets type 3 (VDDR3) through accelerating the metabolic inactivation of vitamin D metabolites. Current treatment relies on sus-tained high-dose vitamin D or calcitriol supplementation, which could not directly correct the pathogenic molecular driver. Traditional therapy such as small-molecule inhibitor or antibody needs complex design and costly screening process, which is considered unsuitable for this kind of rare disease. In the contrast, oligonucleotide therapy offered a more rapid and con-venient screening process. Here, we report the development of an allele-specific small interfering RNA (siRNA) designed to selectively suppress the CYP3A4 I301T mutant transcript while preserving wild-type CYP3A4 expression. A series siRNA candidates with allele-selectivity potential were candidate through rational sequence design. After that the candidates were screened through dual-luciferase reporter assays and four siRNAs displayed strong allelic discrimination were chosen for fur-ther validated. The chemical modifications were employed to improve the biostability and facilitate the hepatocyte-specific delivery (mod-5). The mod-5 exhibited robust allele-specific gene silencing in both dual-luciferase reporter assay and RT-qPCR. Further off-target analysis demonstrated negligible alternation of other CYP450 family transcripts and proteins. Tak-en together, this study establishes an allele-selective RNAi strategy for the treatment of VDDR3 and highlights the potential of small nucleic acid therapeutics for single-nucleotide, gain-of-function rare diseases.

关键词：

siRNA; Allele-Specific; off targeting; Vitamin D Dependent Rickets

目录：

1. Introduction 3
2. Experimental section 4
3. Results and discussion 6
4. Conclusion 16
5. Reference 17

2026 S.T. Yau High School Science Award
仅用于2026丘成桐中学科学奖公示

正文

1. Introduction

Vitamin D-dependent rickets type 3 (VDDR3) is a recently recognized autosomal dominant disorder caused by a gain-of-function from cytochrome P450 3A4 (CYP3A4) single base mutation[1]. In this variant, the thymine at nucleotide position 902 of the CYP3A4 open reading frame is substituted by cytosine (c. T902C), resulting in a replacement of isoleucine to threonine at position 301 (p. I301T). In vitro studies showed that CYP3A4 I301T oxidizes 1,25-dihydroxyvitamin D with markedly higher activity than wild-type CYP3A4[1,2]. Clinically reported cases are characterized by early-onset rickets, reduced levels of 25-hydroxyvitamin D and 1,25-dihydroxyvitamin D, and poor responsiveness to conventional vitamin D supplementation. Only four patients have been documented since the first case was identified in 2018[1,3,4]. The current treatment strategy is therefore largely compensatory: patients require high-dose cholecalciferol, vitamin D analogues, or calcitriol to maintain biochemical remission. Although such therapy improved growth and skeletal manifestations when initiated early, it requires long-term monitoring and does not address the dominant mutant allele that drives accelerated vitamin D degradation[5].

In addition to supplementation, selective inhibition or correction of CYP3A4 I301T are another solution. However, chronic pharmacological inhibition of CYP3A4 may carry substantial drug-drug interaction risks, while small-molecule inhibitors designed to distinguish mutant CYP3A4 I301T from wild-type CYP3A4 are difficult to develop[6,7]. Genome editing approaches such as base editing is conceptually attractive for correcting a single-nucleotide mutation, but delivery, manufacturing complexity, cost, and safety considerations remain major translational barriers, particularly for ultra-rare diseases[8–10].

RNA interference (RNAi) offers a powerful strategy for sequence-directed suppression of disease-causing transcripts[11–13]. During RNAi process, one strand (antisense strand) of the duplex RNA is selectively recognized and loaded into RNA induced silencing complex (RISC). Then, the antisense strand would guide the RISC to bind and cleave complementary targeted mRNA, thereby reducing protein expression at the post-transcriptional level. The fast development of RNAi drugs in the past decades proved the great potential in the treatment of gene disorder diseases[14–19]. Previous studies have demonstrated that siRNAs can discriminate between transcripts differing by a single nucleotide[20–24], offering the opportunity for the selective silencing of CYP3A4 I301T. However, the allelic discrimination is highly dependent on sequence context, the position of the mismatch within the guide strand and local duplex geometry[23]. Therefore, a systematic screening of allele-specific siRNAs is urgently required for the therapeutic intervention of VDDR3.

Here, we reported an allele-specific siRNA targeting the CYP3A4 I301T mutant transcript. Eighteen candidate siRNAs were systematically designed and generated by

2026 S. T. Yau High School Science Award
仅用于2026年丘成桐中学科学奖公示

positioning the mutant nucleotide at positions 2-19 of the antisense strand. Four siRNAs with high allele-selective activity were screened out and a lead siRNA was further selected. Chemical modifications such as 2-OMe and 2-F were introduced to improve the stability of siRNA and $GalNAc_3$ was also conjugated to the sense strand to facilitate the potential liver-targeted delivery. Both dual-luciferase assay and RT-qPCR demonstrated the introduction of chemical modifications improved the gene silencing efficiency. Furthermore, RT-qPCR quantification of mRNA transcripts encoding several CYP3A4 homologous proteins revealed negligible expression alterations. In addition, global proteomic analysis revealed negligible off-target effects. Collectively, this work provides an allele-specific RNAi strategy for the treatment of VDDR3 and supports the broader utility of siRNA therapeutics for rare dominant diseases caused by single-nucleotide gain-of-function mutations.

2. Experimental Methods

2.1 Materials

RNA oligos were purchased from Suzhou Biosyntech Co., Ltd. T4 DNA ligase, XhoI and NotI restriction endonuclease were acquired from New England Biolabs. Lipofectamine™ MessengerMAX™ was acquired from Invitrogen. Dulbecco's modified eagle medium (DMEM), Minimum Essential Medium (MEM), Opti-MEM™ I Reduced Serum Medium and fetal bovine serum (FBS) were purchased from Gibco. Proteinase K and 2X RNA Loading Dye were ordered from Thermo Scientific. FastPure Cell/Tissue Total RNA Isolation Kit V2 and siRNA TransSilent Reagent Pro were purchased from Vazyme. M5 Super plus qPCR RT kit with gDNA remover and 2× M5 HiPer SYBR Premix EsTaq (with Tli RNaseH) were purchased from Mei5bio. QIAquick® PCR Purification Kit was ordered from QIAGEN. Dual-Glo® Luciferase Assay System was acquired from Promega.

2.2 Preparation of siRNA candidates

The concentrations of purchased RNA oligos were determined through NanoDrop according to Lambert-Beer law. The anti-sense strand and sense strand was mixed at 50 μM each in 1×PBS. Then the mixture was heated to 75 °C for 5 min and then cooled to 25 °C at a rate of 0.5 °C/min. The assembled siRNA was characterized through 15% native polyacrylamide gel electrophoresis (PAGE).

2.3 Measurement of siRNA melting temperature

SYBR Green I (Solarbio, SY1020) was diluted to 2× with 1× PBS. Then 10 μL 2×SYBR Green I, 4 μL 2.5 μM siRNA and 6 μL 1× PBS were mixed to obtain a 20 μL mixture per well. The mixture was first kept at 90 °C for 5min and then kept at 25 °C for 5min. After that the temperature was increased to 90 °C at a rate of 0.5 °C/min and the SYBR Green I fluorescent was detected by CFX Connect Real-Time System (Biorad) and the melting temperature was automatically calculated.

2.4 Construction of dual-luciferase reporter plasmid

The double-stranded DNA (dsDNA) containing the CYP3A4 I301T coding sequence, with XhoI and NotI restriction sites introduced at the 5′ and 3′ termini respectively, was

2026 S. T. Yau High School Science Award 应用于2026年丘成桐中学科学奖公示

synthesized by Sangon Biotech (Shanghai) Co., Ltd. The psiCHECK™-2 Vector (Promega, C8021) and dsDNA was then separately cleaved using XhoI (New England Biolabs, R0146V) and NotI (New England Biolabs, R0189V) at 37 °C for 1h. The cleaved products were purified using QIAquick PCR Purification Kit (QIAGEN, 28104). Then the purified products were mixed and ligated using T4 DNA ligase (New England Biolabs, M0202V) to form Mut-reporter plasmid. The WT reporter was constructed by PCR-mediated point mutagenesis of the Mut reporter.

2.5 Evaluation of the silencing efficiency through dual-luciferase reporter assay

293T cells were seeded in 96 well plate at a density of 10^4 cells per well with 100 μL cell culturing medium (DMEM with 10% FBS). After overnight incubation, 10 ng dual-luciferase reporter plasmid (Mut-reporter or WT-reporter) and siRNA at different concentration (10 nM, 1 nM, 0.1 nM and 0.01 nM) were transfected using Lipofectamine™ MessengerMAX™ (Invitrogen™, LMRNA015) according to the manufacturer's instructions. The cells continued to culture under conditions of 37°C and 5% CO_2. 24 h after transfection, the activity of firefly luciferase and Renilla luciferase were measure using Dual-Glo® Luciferase Assay System (E2920). Briefly, the medium was exchanged to 60 μL cell culturing medium, and 60 μL Dual-Glo® Luciferase Assay Reagent was added. Then the mixture was incubated at room temperature for 10 min and transferred to a white bottom 96 well plate. The firefly luciferase activity was measured through plate reader. After that, 60 μL freshly prepared Dual-Glo® Stop & Glo® Reagent was added, and the mixture was incubated at room temperature for 10 min. Then the Renilla luciferase activity was measure through plate reader. The relative luminescence was used to quantify the gene silencing efficiency.

2.6 Evaluation of the silencing efficiency through real-time quantitative PCR

293T cells were seeded in 12 well plate at a density of 2.5×10^5 cells per well with 1 mL cell culturing medium (DMEM with 10% FBS). After overnight incubation, 100 ng dual-luciferase reporter plasmid (Mut-reporter or WT-reporter) and siRNA at different concentration (10 nM, 1 nM, 0.1 nM and 0.01 nM) were transfected using Lipofectamine™ MessengerMAX™ (Invitrogen™, LMRNA015) according to the manufacturer's instructions. The cells continued to culture under conditions of 37°C and 5% CO_2. 24 h after transfection, cells were harvested for subsequent total RNA isolation and RT-qPCR.

2.7 Total RNA isolation and real-time quantitative PCR

The total RNA was isolated using FastPure Complex Tissue/Cell Total RNA Isolation Kit (Vazyme, RC113-01) according to the manufacturer's instructions. 1 μg total RNA was used for cDNA synthesis using M5 Super plus qPCR RT kit with gDNA remover (Mei5bio, MF166-plus-01). Then the real-time PCR was performed using 2X M5 HiPer SYBR Premix EsTaq (with Tli RNaseH) (Mei5bio, MF787-NR-01) according to the manufacturer's instructions through CFX Connect Real-Time System (Biorad). For 293T cells the relative expression level of Rluc mRNA was normalized to Fluc mRNA. For HepG2 cells, the relative expression level of CYP3A4, CYP3A5, CYP3A7, CYP2C9, CYP2D6 mRNA were normalized to GAPDH mRNA. All the data were analyzed using GraphPad Prism 9.

2026 S.T. Yau High School Science Award
项目编号2026王诗宗科学奖公示

2.8 Evaluation of the biostability

200 pmol mod-5 and siRNA 5 were mixed with DMEM contained 10% FBS to a final volume of 50 μL. Then the mixture was incubated at 37°C. 5 μL sample was collected at different time points (0h, 0.5h, 1h, 6h, 12h, 24h, 48h, 72h and 96h) and mixed with 2 μL Proteinase K (Thermo Scientific™, EO0491). Then the mixture was heated to 50°C and kept for 5 min to inactive the FBS. 2 μL sample was mixed with 3 μL 2X RNA Loading Dye and analyzed through 15% native PAGE.

2.9 Evaluation of off-target silencing of CYP family mRNA

HepG2 cells were seed in 12 well plate at a density of 4×10^5 cells per well with 1 mL cell culturing medium (DMEM with 10% FBS). After overnight incubation, mod-5 or mod-R was transfected at 10 nM concentration using siRNA TransSilent Reagent Pro (Vazyme, TL101) according to the manufacturer's instructions. The cells continued to culture under conditions of 37°C and 5% CO_2. 24 h after transfection, cells were harvested for subsequent total RNA isolation and RT-qPCR.

2.10 Proteome off-target analysis

HepG2 cells were seed in 6 well plate at a density of 1×10^6 cells per well with 2 mL cell culturing medium (DMEM with 10% FBS). After overnight incubation, mod-5 or mod-R was transfected at 10 nM concentration using siRNA TransSilent Reagent Pro (Vazyme, TL101) according to the manufacturer's instructions. The cells continued to culture under conditions of 37°C and 5% CO_2. Cells were harvested 48 h after transfection for proteomic analysis.

3. Result and Discussion

3.1 Design and characterization of siRNA candidates

To discriminate the single-base mutation in CYP3A4 I301T transcript, we designed a series siRNA with antisense strand (AS) complementary to the mutant mRNA. Several design rules were carefully considered according to the mechanism of RNAi[25] (Figure 1A): 1) The 5'-terminal nucleoside determines selective loading of the AS into Ago2, and adenosine or uridine residues are favored at this position. 2) The seed region (positions 2-8) shapes the Ago2 binding pocket to mediate mRNA recognition, and nucleotides within this segment dominate the sequence specificity of RNAi. 3) The cleavage core (positions 9-11) governs catalytic hydrolysis of phosphodiester bonds in target transcripts and a single-base mismatch within this region may be sufficient to abolish RISC cleavage activity. 4) The 3' supplementary region (positions 12-19) stabilizes full-length duplex formation following seed-region hybridization and improves selectivity of RNAi. 5) The 2-nucleotide 3' overhang is captured by the PAZ domain of Ago2 to anchor the AS within RISC, whereas the base composition of this overhang exerts no influence on RISC target recognition. Taken together, the bases between position 2-19 are important for the sequence specificity of RNAi and no generalized guideline for rational allele-specific siRNA design has been proposed to date.

2026 S.T. Yau High School Science Award
仅用于2026丘成桐中学科学奖论文公示

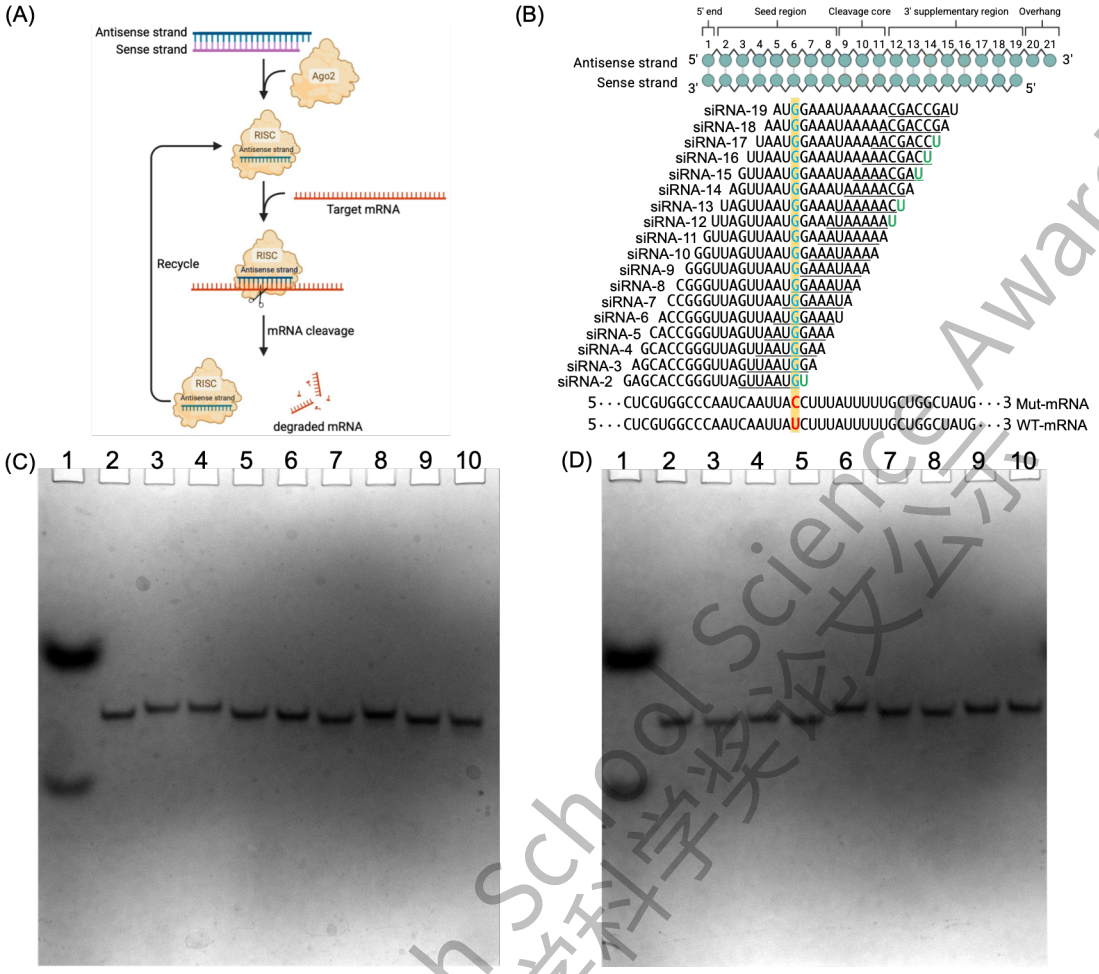


Figure 1 Design and synthesis of siRNAs. (A) Scheme illustrated of the designed siRNA-2 to siRNA-19. Underline: seed region; Blue: mutation site; Green: unpaired base. (B) 15% native PAGE analysis of synthesized siRNA. Lane 1 to 10: Loading, siRNA-2, siRNA-3, siRNA-4, siRNA-5, siRNA-6, siRNA-7, siRNA-8, siRNA-9, siRNA-10. (C) 15% native PAGE analysis of synthesized siRNA. Lane 1 to 10: Loading, siRNA-11, siRNA-12, siRNA-13, siRNA-14, siRNA-15, siRNA-16, siRNA-17, siRNA-18, siRNA-19.

Table 1 sequences of 18 unmodified siRNA candidates

Name		Sequence 5' to 3'	Length
siRNA-2	Anti-sense	UGUAAUUGAUUGGGCCACGAG	21
	Sense	CGUGGCCCAAUCAAUUACA	19
siRNA-3	Anti-sense	AGGUAAUUGAUUGGGCCACGA	21
	Sense	GUGGCCCAAUCAAUUACCU	19
siRNA-4	Anti-sense	AAGGUAAUUGAUUGGGCCACG	21
	Sense	UGGCCCAAUCAAUUACCUU	19
siRNA-5	Anti-sense	AAAGGUAAUUGAUUGGGCCAC	21
	Sense	GGCCCAAUCAAUUACCUUU	19

2026 S-T Youth School Science Award
仅用于2026年成都中学科学奖论文公示

siRNA-6	Anti-sense	UAAAGGUAAUUGAUUGGGCCA	21
	Sense	GCCCAAUCAAUUACCUUUA	19
siRNA-7	Anti-sense	AUAAAGGUAAUUGAUUGGGCC	21
	Sense	CCCAAUCAAUUACCUUUAU	19
siRNA-8	Anti-sense	AAUAAAGGUAAUUGAUUGGGC	21
	Sense	CCAAUCAAUUACCUUUAUU	19
siRNA-9	Anti-sense	AAAUAAAGGUAAUUGAUUGGG	21
	Sense	CAAUCAAUUACCUUUAUUU	19
siRNA-10	Anti-sense	AAAAUAAAGGUAAUUGAUUGG	21
	Sense	AAUCAAUUACCUUUAUUUU	19
siRNA-11	Anti-sense	AAAAAUAAAGGUAAUUGAUUG	21
	Sense	AUCAAUUACCUUUAUUUUU	19
siRNA-12	Anti-sense	UAAAAAUAAAGGUAAUUGAUU	21
	Sense	UCAAUUACCUUUAUUUUUA	19
siRNA-13	Anti-sense	UCAAAAAUAAAGGUAAUUGAU	21
	Sense	CAAUUACCUUUAUUUUUGA	19
siRNA-14	Anti-sense	AGCAAAAAUAAAGGUAAUUGA	21
	Sense	AAUUACCUUUAUUUUUGCU	19
siRNA-15	Anti-sense	UAGCAAAAAUAAAGGUAAUUG	21
	Sense	AUUACCUUUAUUUUUGCUA	19
siRNA-16	Anti-sense	UCAGCAAAAAUAAAGGUAAUU	21
	Sense	UUACCUUUAUUUUUGCUGA	19
siRNA-17	Anti-sense	UCCAGCAAAAAUAAAGGUAAU	21
	Sense	UACCUUUAUUUUUGCUGGA	19
siRNA-18	Anti-sense	AGCCAGCAAAAAUAAAGGUAA	21
	Sense	ACCUUUAUUUUUGCUGGCU	19
siRNA-19	Anti-sense	UAGCCAGCAAAAAUAAAGGUA	21
	Sense	CCUUUAUUUUUGCUGGCUA	19

Based on the rules mentioned above, eighteen siRNA candidates (sequences were shown in Table 1) were designed for subsequent screening. As shown in Figure 1B, each of siRNA 2-19 contains a single-base mismatch (G: U mismatch) against wild type (WT) mRNA at different positions. In some cases, the 5'-terminal of the AS would be cytosine or guanine, which might impair effectively assembly of RISC. Thus, uridine was used to replace the C or G in these cases. Furthermore, the asymmetry structure was used to facilitate the corrected loading of AS to RISC instead of off-targeted SS loading: 21nt AS and 19nt sense strand (SS), with 2nt single strand overhang at the 3-end of AS.

In our study, the AS and SS were synthesized via solid-phase chemical synthesis and purified separately. Then the AS and corresponding SS was mixed at the molar ratio of

2026 S_T Yau Hiwin School Science Award
仅用于2026丘成桐科学奖论文公示

1:1 and assembled through annealing. The integrity of siRNAs was analyzed through native polyacrylamide gel electrophoresis (PAGE). The single clear band in each lane of Figure 1C and D demonstrated the successful preparation of siRNA 2-19. Slight differences in migration rates could be attributed to distinct secondary structures caused by varying nucleotide sequences. The melting temperature (Tm) of the designed siRNA were also measured. As shown in Figure 2A, the Tm of siRNA duplex firstly decreased form siRNA 2 to 10 and then increased from siRNA 12 to 19. Notably, the Tm of each siRNA duplex showed a parallel tendency to GC content (Figure 2B), demonstrating that higher GC proportions strengthened duplex thermal stability. Moreover, the Tm of all eighteen siRNA candidates was higher than 50 °C, suggesting stable base pairing between AS and target mRNA, which is beneficial to the robust gene silencing efficiency.

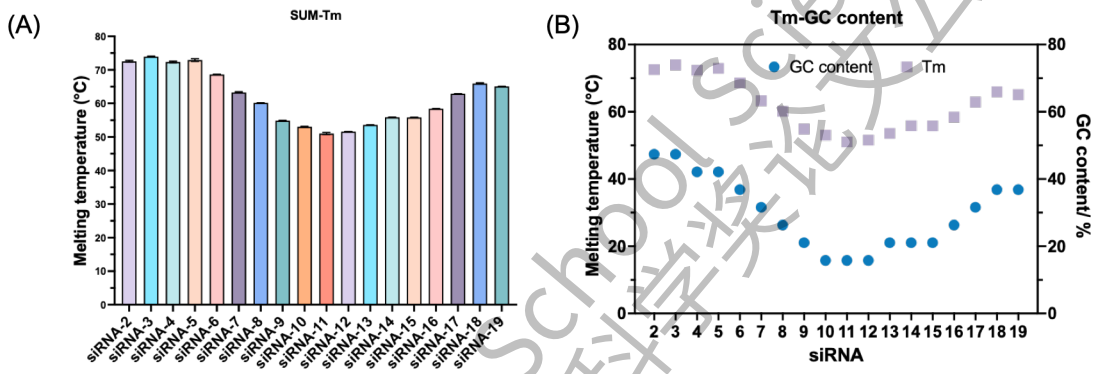


Figure 2 Melting temperature of designed siRNA candidates measured through SYBR Green I with qPCR machine. (A) Tm of the siRNA candidates. (B) Relationship between Tm and GC content of the siRNA candidates.

3.2 Design and construction of dual-luciferase reporter plasmid

The 293T cells were used to assess the allele-specificity of designed siRNA 2-19 through dual-luciferase reporter assay (Figure 3A). Two different luciferase, *Renilla* luciferase (Rluc) and firefly luciferase (Fluc), were introduced downstream of different promoter. The coding sequence (CDS) of either mutant (Mut) (Figure 3A, left) or WT CYP3A4 (Figure 3A, right) was inserted downstream of the stop codon of Rluc, which act as the 3'-untranslated region and no fusion protein would be expressed. After the co-transfection of the reporter plasmid and siRNA candidate, the AS would load to the endogenous Ago2 and formed RISC. If the RISC could recognize the insert sequence and initiates the RNAi process, the fused Rluc-CDS mRNA will be cleavage and degraded, which further decrease the activity of Rluc. Meanwhile, Fluc serves as an internal control, unaffected by siRNA candidates, enabling normalized quantification of the gene silencing efficiency through the normalized ratio of Rluc to Fluc.

3.3 Screening siRNA candidates through dual-luciferase reporter assay

2026 Yau Hing School Science Award 仅用于2026年油麻地科学奖论文公示

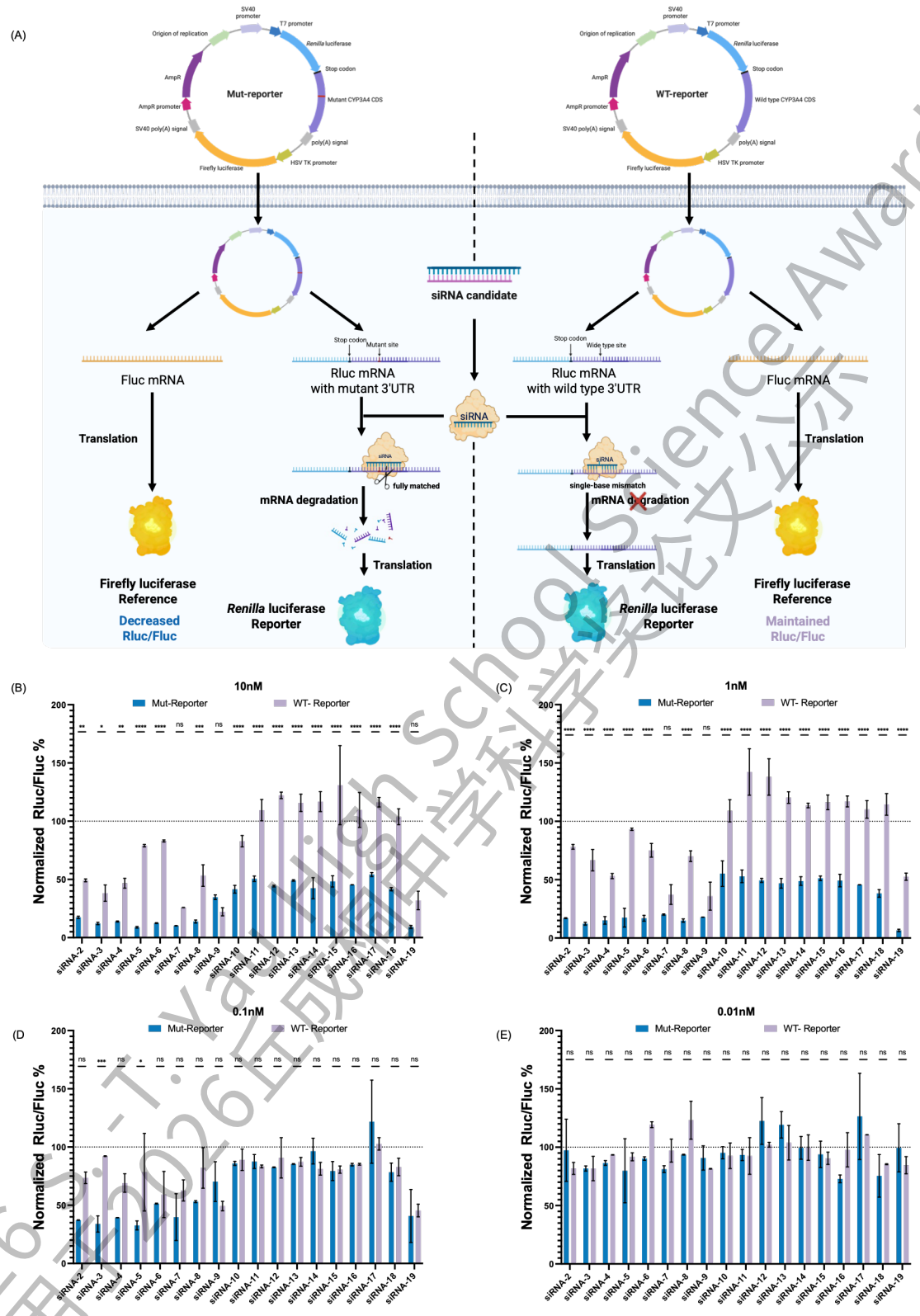


Figure 3 Screening of the RNAi efficiency of designed siRNA through dual-luciferase assay. (A) Design of the dual-luciferase assay with mutant or wild type CYP3A4 CDS. (B)-(E) Normalized Rluc/Rluc in 293T cell transfected with dual-luciferase reporter plasmid and siRNA 2-19 at 10nM (B), 1nM(C), 0,1nM(D), 0.01nM(E). Three independent experiments were performed, and multiple comparisons were performed

2026 Y-I Yat Hin School Science Award
仅用于2026亿成中学科学奖论文公示

using one-way ANOVA with Tukey's test. *P < 0.05, **P < 0.01, and ***P < 0.001, ****P < 0.0001.

At 10nM (Figure 3B), siRNA 2-8 and siRNA 19 achieved over 80% silencing efficiency against mutant CDS, whereas siRNA 9-18 exerted moderate repression of the mutant transcript. This silencing efficiency trend aligned with the Tm variations presented in Figure 2: siRNA 2 to siRNA 8 and siRNA 19 possessed higher Tm than the other candidates. At the same time, siRNA 11-18 exhibited nearly negligible suppression against the wild-type reporter plasmid at 10nM, while siRNA 5 and 6 showed less than 20% knockdown. Collectively, these data demonstrate that single-base mismatches can effectively compromise siRNA mediated gene silencing, and such effects exhibit strong positional dependence. The mismatch located within seed region drastically impaired silencing toward WT mRNA, endowing siRNA 5 and 6 with robust allele selectivity. Furthermore, mismatch at 3' supplementary region reduced the thermostability of RISC-mRNA duplex and showed allele selectivity, such as siRNA 11-18. Interestingly, mismatch at cleavage core (siRNA 9 and 10) did not showed specificity to mutant CDS to WT, probably because of the G:U base pairing was tolerant at this region. A consistent inhibitory profile was observed at 1nM (Figure 3C).

At lower concentration, the silencing efficiency was decreased. siRNA 2-9 moderately inhibited mutant CDS with weaker repression toward wild-type CDS and siRNA 10-19 produced indistinguishable inhibitory effects on mutant and wild-type transcripts at 0.1nM (Figure 3D). Moreover, only siRNA 2 and siRNA 5 exhibited statistically significant differences in silencing activity between Mut and WT reporter constructs at 0.1nM. At the lowest tested concentration (0.01nM, Figure 3E), none of the candidate siRNAs induced obvious repression of either mutant or WT CDS. Given the robust allelic discrimination capacity of siRNA 5, siRNA 6, siRNA 15 and siRNA 16 across all tested concentrations, their sequences were selected for subsequent functional experiments.

3.4 Direct measurement of silencing efficiency through RT-qPCR

Next, we further evaluated the gene silencing efficiency of siRNA 5, 6, 15 and 16 *via* real-time quantitative PCR (RT-qPCR). As shown in Figure 4A, 293T cells were co-transfected with plasmids carrying either mutant or wild-type CYP3A4 CDS and serially diluted siRNAs. Cells were harvested and lysed at 24 h post-transfection. Rluc mRNA levels were quantified, with Fluc mRNA serving as an internal control to normalize variations in transfection efficiency.

Notably, the mRNA expression profiles did not fully correlate with the dual-luciferase activity results. For instance, at 10 nM, siRNA 15 and 16 exhibited approximately 50% silencing in the reporter assay, whereas no obvious reduction was detected at the mRNA level (Figure 4B). This discrepancy indicates that these siRNAs primarily exert effects through translational repression, rather than direct cleavage and degradation of target mRNA. On the contrary, siRNA 5 and 6 showed significant suppression of mRNA level. As depicted in Figure 3B and C, siRNA 5 and 6 showed around 55% mRNA inhibition at 10nM and around 50% inhibition at 1nM, indicated the decreased Rluc activity in

2026 S.T. Yau High School Science Award
仅用于2026三叉桐中学科学奖论文公示

Figure 3B and C was preliminary due to the mRNA degradation. Similar potency was also observed at low concertation (Figure 4D and E). Meanwhile, all the four candidates showed no significant inhibition against WT-CDS mRNA, which demonstrated the single-base mismatch efficiently abolished the RISC cleavage. As the siRNA 5 showed highest allelic discrimination capacity and robust inhibition against mutant CYP3A4 CDS, this sequence was chosen for subsequence experiments.

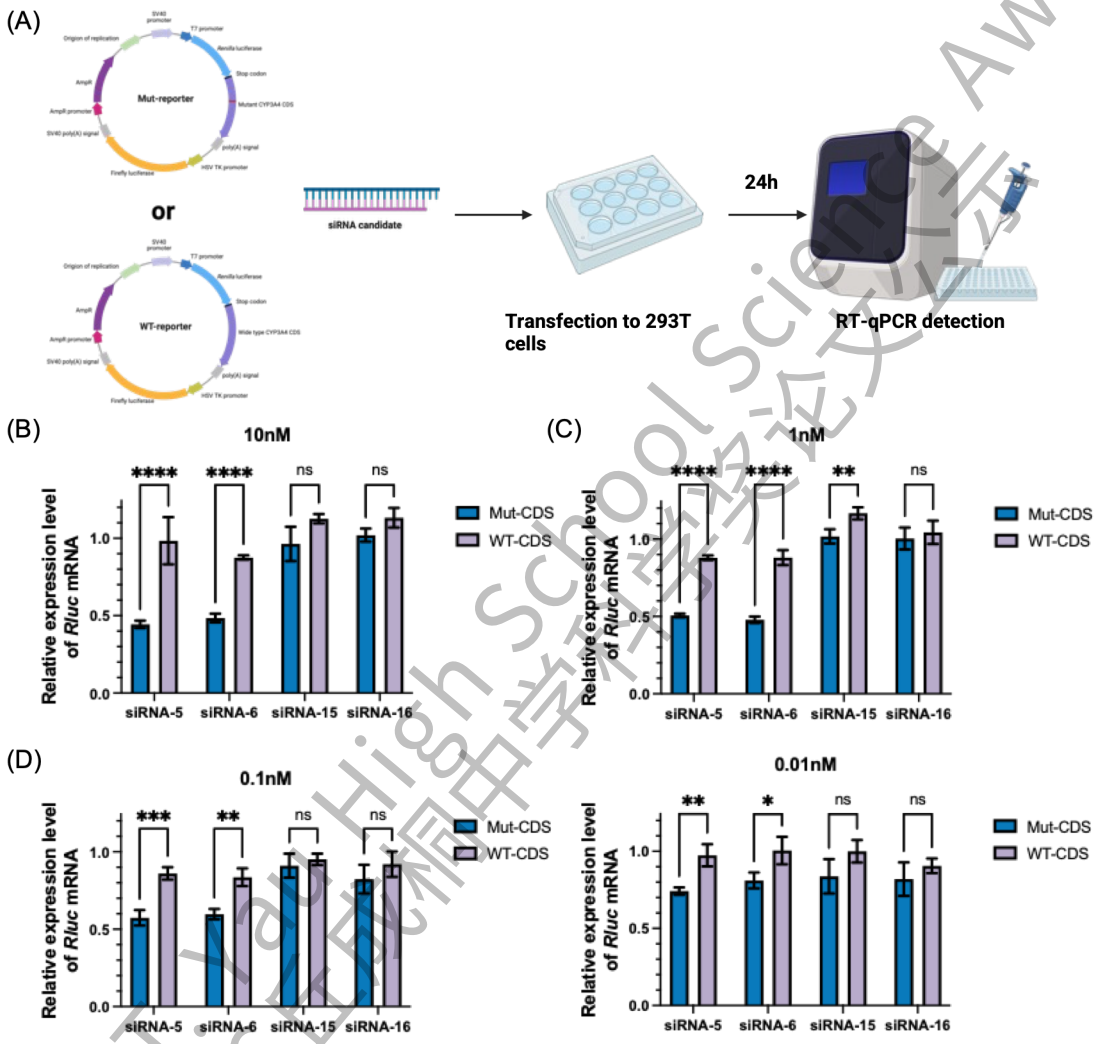


Figure 4 Evaluation of the mRNA silencing efficiency of four selected siRNA candidates through RT-qPCR. (A) Direct measurement of mRNA silencing efficiency through RT-qPCR in 293T cells. (B) mRNA silencing efficiency against Mut-CDS or WT-CDS with siRNA-5, 6, 15, 16 at 10nM. (C) mRNA silencing efficiency against Mut-CDS or WT-CDS with siRNA-5, 6, 15, 16 at 1nM. (D) mRNA silencing efficiency against Mut-CDS or WT-CDS with siRNA-5, 6 at 0.1nM. (E) mRNA silencing efficiency against Mut-CDS or WT-CDS with siRNA-5, 6 at 0.01nM. The mRNA expression was measured through RT-qPCR using Fluc as the internal control. Data represent at least three independent experiments, with multiple comparisons performed using one-way ANOVA followed by Tukey's test. *P < 0.05, **P < 0.01, ***P <0.001, and ****P < 0.0001.

2026 Tianjin High School Science Award 仅用于2026年天津高中科学奖论文评选

3.5 Design and validation of chemically modified siRNA

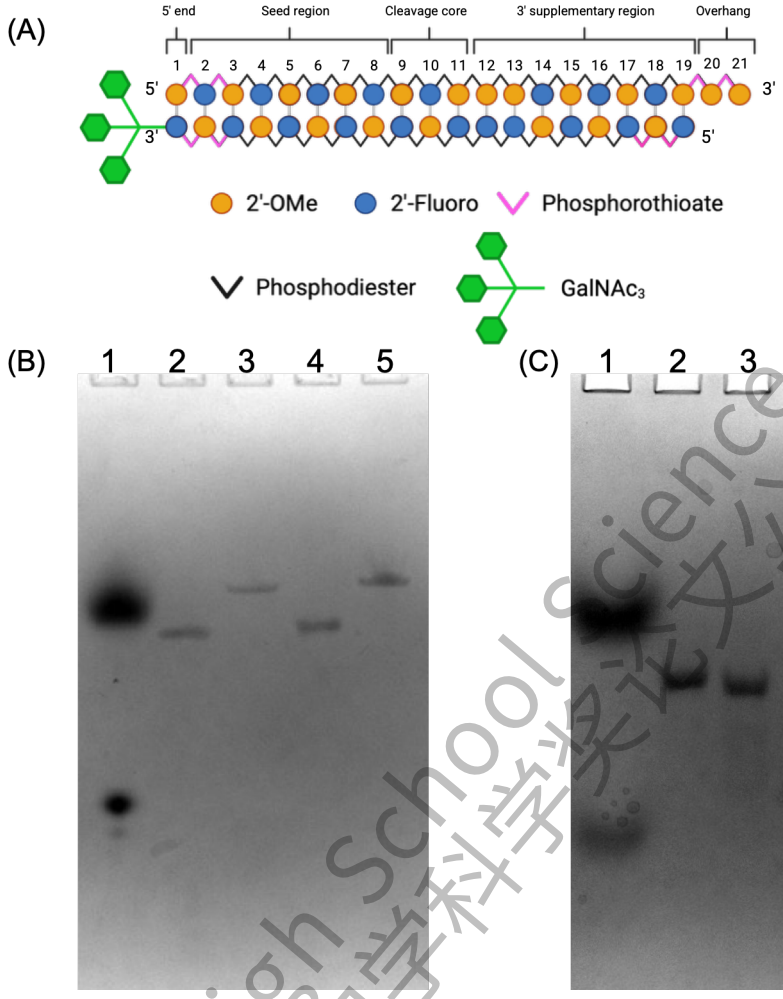


Figure 5 Design and synthesis of chemically modified siRNA. (A) Chemically modified patterns used in mod-5 and mod-R. (B) 20% denaturing polyacrylamide gel electrophoresis (PAGE) analysis of the chemically synthesized siRNA. Lane 1 to 5: Loading; mod-5-AS; mod-5-SS-Gal; mod-R-AS; mod-R-SS-Gal. (C) 15% native PAGE analysis of the assembled mod-5 and mod-R.

Next, chemicals modifications were introduced to enhance the biostability and facilitate hepatocyte-target delivery. As shown in Figure 5A, terminal phosphorothioate (PS) can protected the siRNA from the degradation by exonucleases and site-specific 2'-fluoro (2'-F) and 2'-O-methyl (2'-OMe) modifications can enhance the binding affinity and decreased the immunogenicity. Furthermore, as the CYP3A4 was preliminary expressed in hepatocyte, *N*-acetyl galactosamine trimer ($GalNAc_3$) was introduced to the 3'-end of sense strand to facilitate hepatocyte-specific delivery (mod-5)[26,27]. The purity of chemical modified siRNA was first validated through PAGE. As shown in Figure 5B and 5C, the clear band in both denaturing and native PAGE demonstrated the high purity of synthesized modified siRNA. Then the unmodified siRNA 5 and modified mod-5 were incubated with 10% FBS at 37°C. Samples were collected at different time points and analyzed through 15% native PAGE. As shown in Figure 6, siRNA 5 gradually degradation while mod-5 remains intact even after 96 hours.

2026 S. T. Yau High School Science Award
仅用于2026丘成桐中学科学奖公示

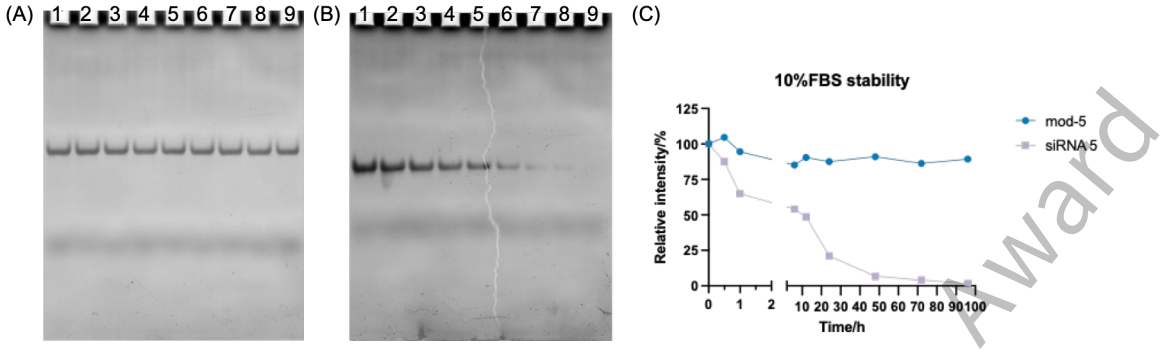


Figure 6 Biostability evaluation of the modified mod-5 and unmodified siRNA 5 in DMEM contains 10% FBS. (A) 15% native PAGE analysis of the mod-5 incubated for different times. Lane 1 to 9: mod-5 incubated with DMEM contains 10% FBS for 0h, 0.5h, 1h, 6h, 12h, 24h, 48h, 72h and 96h. (B) 15% native PAGE analysis of the siRNA 5 incubated for different times. Lane 1 to 9: siRNA 5 incubated with DMEM contains 10% FBS for 0h, 0.5h, 1h, 6h, 12h, 24h, 48h, 72h and 96h. (C) Quantitative result of A and B through Image J.

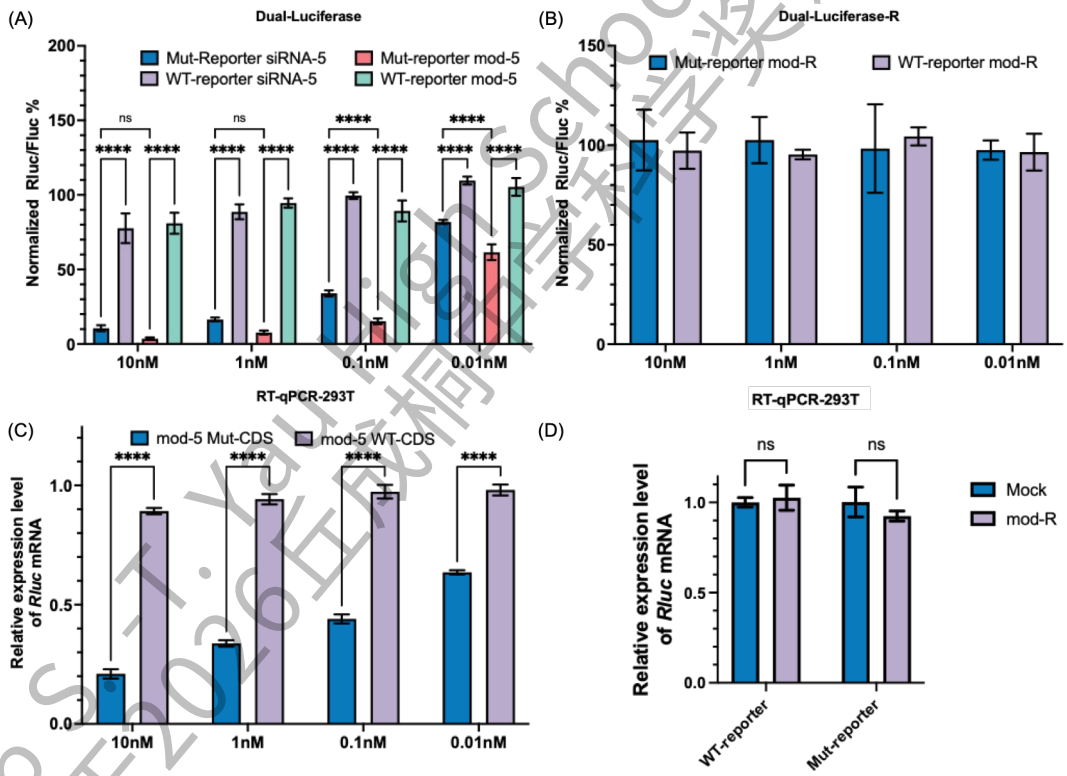


Figure 7 Evaluation of the chemical modified siRNA gene silencing efficiency(A) Dual-luciferase reporter assay evaluation of the gene silencing efficiency of siRNA-5 and mod-5 against Mut-CDS or WT-CDS in 293T cells at different concentrations. (B) Dual-luciferase reporter assay evaluation of the gene silencing efficiency of mod-R against Mut-CDS or WT-CDS in 293T cells at different concentrations. (C) RT-qPCR analysis mRNA silencing efficiency against Mut-CDS or WT-CDS with mod-5 in 293T cells at different concentrations. (D) RT-qPCR analysis mRNA silencing efficiency of

2026 S.T. Yau High School Science Award
仅用于2026丘成桐中学科学奖论文公开

mod-R against Mut-CDS or WT-CDS with mod-5 and mod-R in 293T cells at 10nM. Three independent experiments were performed, with multiple comparisons performed using one-way ANOVA followed by Tukey's test. *P < 0.05, **P < 0.01, ***P <0.001, and ****P < 0.0001.

Dual-luciferase reporter assays were then performed to evaluate the silencing activity of modified siRNAs. As shown in Figure 7A, mod-5 showed higher silencing efficiency against Mut-CDS compared with unmodified siRNA 5 across all tested concentrations, with significant improvement at 0.1nM and 0.01nM. This improvement can be attributed to enhanced biostability and mRNA-binding affinity conferred by designed chemical modifications as the siRNA with random sequence and the same modification pattern (mod-R) showed no inhibitions (Figure 7B). At the same time, the mod-5 retains the single-base discrimination during gene silencing similar to siRNA 5. Furthermore, RT-qPCR results (Figure 7C and 7D) also confirmed the robust allele-specific knockdown against mutant CDS of mod-5, while mod-R exhibited negligible changes. Taken together, these results demonstrated the designed mod-5 allele-specific silencing capability and had higher silencing efficiency against mutant CDS.

3.6 Evaluation of the off-target effects

The selectivity of mod-5 was further evaluated in HepG2 cells. The cytochrome P450 superfamily consists of multifunctional metabolic enzymes ubiquitously distributed across living organisms and CYP450s mediated approximately 75% of all clinical drug metabolic reactions[28]. For example, CYP3A5 exists high sequence similarity (~84%) with CYP3A4. The off-target inhibition of the CYP450s may disrupt the homeostasis of hepatic drug-metabolizing networks which further could induce metabolic disorder and potential cytotoxicity and unpredictable cellular adverse effects. 24 hours after transfection with 10nM mod-5 or mod-R, mRNA expression levels of CYP3A subfamily (wild type CYP3A4, CYP3A5, CYP3A7, CYP3A43) and two representative phase I metabolic enzymes (CYP2C9 and CYP2D6) were quantitated. As shown in Figure 8A, no detectable changes in the expression of selected homologous transcripts were observed for either mod-5 or mod-R. Hence, the chemically modified mod-5 exhibits high selectivity toward mutant CYP3A4.

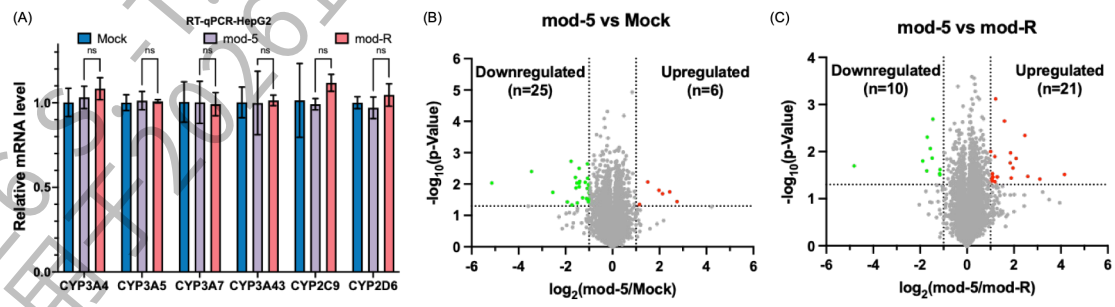


Figure 8 Evaluation of the off-target effects of chemically modified siRNA. (A) Relative mRNA expression level of CYP3A4, CYP3A5, CYP3A7, CYP3A43, CYP2C9, CYP2D6 in HepG2 cells after transfection with 10nM mod-5 and mod-R. (B) Proteomic analysis of HepG2 cells 48h after transfecting with 10nM mod-5 or Mock. (B) Proteomic analysis of HepG2 cells 48h after transfecting with 10nM mod-5 or mod-

R. The mRNA expression was measured through RT-qPCR using GAPDH as the internal control. Data represent at least three independent experiments, with multiple comparisons performed using one-way ANOVA followed by Tukey's test. *P < 0.05, **P < 0.01, ***P <0.001, and ****P < 0.0001.

To further elucidate the global cellular perturbations induced by the designed siRNA at the protein level, proteomic profiling was performed from three experimental groups: mock group, mod-R group, and mod-5 group. Differential expression analysis and functional enrichment of the proteome dataset were conducted to systematically verify whether mod-5 caused widespread off-target silencing across the CYP450 family or disrupted the homeostasis of the hepatic metabolic network. Figure 8B (mod-5 vs mock) and Figure 8C (mod-5 vs mod-R) showed minimal alteration of the HepG2 proteome. Notably, the detected CYP450 family proteins and immunogenicity-related proteins showed no difference between mod-5 and mock group, indicated the high specificity and low immunogenicity of designed chemical modified siRNA.

4. Conclusion

In summary, we systematically screened eighteen allele-specific siRNA candidates targeting the pathogenic CYP3A4 I301T mutant linked to VDDR3. Through dual-luciferase reporter screening and RT-qPCR validation, siRNA 5 was selected as the optimal candidate owing to its potent and selective silencing of mutant transcripts while showing minimal affect to wild-type CYP3A4. After that, chemical modifications such as 2'-F, 2'-OMe, PS and GalNAc conjugation were introduced to enhance biostability, reduce immunogenicity and enable liver-targeted delivery. The chemically modified siRNA retained robust allele-specific activity. Further off-target assessments revealed that mod-5 exerted negligible impacts on closely homologous CYP3A subfamily members (CYP3A5, CYP3A7, CYP3A43) and other major drug-metabolizing CYP isoforms (CYP2C9, CYP2D6) at the mRNA level. Global proteomic analysis also confirmed its safety and minimal disturbance to hepatic metabolic networks. Collectively, this work provides a promising RNAi therapeutic candidate for VDDR3 and offers a feasible strategy for developing allele-selective siRNAs against single-nucleotide gain-of-function genetic disorders.

2026 S. T. Yau High School Science Award
仅用于2026丘成桐中学科学奖论文公示

Reference

(1) Roizen, J. D.; Li, D.; O'Lear, L.; Javaid, M. K.; Shaw, N. J.; Ebeling, P. R.; Nguyen, H. H.; Rodda, C. P.; Thummel, K. E.; Thacher, T. D.; Hakonarson, H.; Levine, M. A. CYP3A4 Mutation Causes Vitamin D–Dependent Rickets Type 3. *J. Clin. Invest.* **2018**, *128* (5), 1913–1918. https://doi.org/10.1172/JCI98680.

(2) Nakaya, N.; Sakamoto, R.; Mano, H.; Mikami, B.; Imaishi, H.; Nagasawa, K.; Sakaki, T.; Yasuda, K. Distinct and Potent Vitamin D Hydroxylation Activity Acquired by the CYP3A4 I301T Single Amino Acid Substitution Causes Type 3 Rickets. *FEBS J.* **2026**, *293* (3), 660–676. https://doi.org/10.1111/febs.70277.

(3) Al-Ashwal, A.; Al Zahrani, A.; Dammas, N.; Aletani, L.; Alhuthil, R. CYP3A4 Mutation Causes Vitamin D-Dependent Rickets Type 3: A Case Report in Saudi Arabia. *Cureus* **2023**, *15* (12), e49976. https://doi.org/10.7759/cureus.49976.

(4) Mantoanelli, L.; de Almeida, C. M.; Coelho, M. C. A.; Coutinho, M.; Levine, M. A.; Collett-Solberg, P. F.; Bordallo, A. P. Vitamin D-Dependent Rickets Type 3: A Case Report and Systematic Review. *Calcif. Tissue Int.* **2023**, *112* (4), 512–517. https://doi.org/10.1007/s00223-022-01051-2.

(5) Sarathi, V.; Dhananjaya, M. S.; Karlekar, M.; Lila, A. R. Vitamin D Deficiency or Resistance and Hypophosphatemia. *Best Pract. Res. Clin. Endoc. Metab.* **2024**, *38* (2), 101876. https://doi.org/10.1016/j.beem.2024.101876.

(6) Lee, J.; Park, S. B. Extended Applications of Small-Molecule Covalent Inhibitors toward Novel Therapeutic Targets. *Pharmaceuticals* **2022**, *15* (12), 1478. https://doi.org/10.3390/ph15121478.

(7) Wang, J.; Nithianantham, S.; Chai, S. C.; Jung, Y.-H.; Yang, L.; Ong, H. W.; Li, Y.; Zhang, Y.; Miller, D. J.; Chen, T. Decoding the Selective Chemical Modulation of CYP3A4. *Nat. Commun.* **2025**, *16* (1), 3423. https://doi.org/10.1038/s41467-025-58749-8.

(8) Zhong, Z.; Guo, J.; Deng, L.; Chen, L.; Wang, J.; Li, S.; Xu, W.; Deng, Z.; Sun, Y. Base Editing in Streptomyces with Cas9-Deaminase Fusions. *bioRxiv* **2019**, 630137. https://doi.org/10.1101/630137.

(9) Porto, E. M.; Komor, A. C.; Slaymaker, I. M.; Yeo, G. W. Base Editing: Advances and Therapeutic Opportunities. *Nat. Rev. Drug Discov.* **2020**, *19* (12), 839–859. https://doi.org/10.1038/s41573-020-0084-6.

(10) Lin, Q. Prime Editing: Redefining Precision Genome Editing. *Nat. Rev. Genet.* **2026**, *27* (8), 583–583. https://doi.org/10.1038/s41576-026-00965-z.

(11) Crooke, S. T.; Baker, B. F.; Crooke, R. M.; Liang, X. Antisense Technology: An Overview and Prospectus. *Nat. Rev. Drug Discov.* **2021**, *20* (6), 427–453. https://doi.org/10.1038/s41573-021-00162-z.

(12) Kole, R.; Krainer, A. R.; Altman, S. RNA Therapeutics: Beyond RNA Interference and Antisense Oligonucleotides. *Nat. Rev. Drug Discov.* **2012**, *11* (2), 125–140. https://doi.org/10.1038/nrd3625.

(13) Jadhav, V.; Vaishnaw, A.; Fitzgerald, K.; Maier, M. A. RNA Interference in the Era of Nucleic Acid Therapeutics. *Nat. Biotechnol.* **2024**, *42* (3), 394–405. https://doi.org/10.1038/s41587-023-02105-y.

2026 S. T. Yau High School Science Award 仅用于2026丘成桐中学科学奖公示

(14) Setten, R. L.; Rossi, J. J.; Han, S. The Current State and Future Directions of RNAi-Based Therapeutics. *Nat. Rev. Drug Discov.* **2019**, *18* (6), 421–446. https://doi.org/10.1038/s41573-019-0017-4.

(15) Brown, K. M.; Nair, J. K.; Janas, M. M.; Anglero-Rodriguez, Y. I.; Dang, L. T. H.; Peng, H.; Theile, C. S.; Castellanos-Rizaldos, E.; Brown, C.; Foster, D.; Kurz, J.; Allen, J.; Maganti, R.; Li, J.; Matsuda, S.; Stricos, M.; Chickering, T.; Jung, M.; Wassarman, K.; Rollins, J.; Woods, L.; Kelin, A.; Guenther, D. C.; Mobley, M. W.; Petrulis, J.; McDougall, R.; Racie, T.; Bombardier, J.; Cha, D.; Agarwal, S.; Johnson, L.; Jiang, Y.; Lentini, S.; Gilbert, J.; Nguyen, T.; Chigas, S.; LeBlanc, S.; Poreci, U.; Kasper, A.; Rogers, A. B.; Chong, S.; Davis, W.; Sutherland, J. E.; Castoreno, A.; Milstein, S.; Schlegel, M. K.; Zlatev, I.; Charisse, K.; Keating, M.; Manoharan, M.; Fitzgerald, K.; Wu, J.-T.; Maier, M. A.; Jadhav, V. Expanding RNAi Therapeutics to Extrahepatic Tissues with Lipophilic Conjugates. *Nat. Biotechnol.* **2022**, *40* (10), 1500–1508. https://doi.org/10.1038/s41587-022-01334-x.

(16) Wang, F.; Xie, M.; Huang, Y.; Liu, Y.; Liu, X.; Zhu, L.; Zhu, X.; Guo, Y.; Zhang, C. In Situ Vaccination with An Injectable Nucleic Acid Hydrogel for Synergistic Cancer Immunotherapy. *Angew. Chem. Int. Ed.* **2024**, *63* (4), e202315282. https://doi.org/10.1002/anie.202315282.

(17) Alterman, J. F.; Godinho, B. M. D. C.; Hassler, M. R.; Ferguson, C. M.; Echeverria, D.; Sapp, E.; Haraszti, R. A.; Coles, A. H.; Conroy, F.; Miller, R.; Roux, L.; Yan, P.; Knox, E. G.; Turanov, A. A.; King, R. M.; Gernoux, G.; Mueller, C.; Gray-Edwards, H. L.; Moser, R. P.; Bishop, N. C.; Jaber, S. M.; Gounis, M. J.; Sena-Esteves, M.; Pai, A. A.; DiFiglia, M.; Aronin, N.; Khvorova, A. A Divalent siRNA Chemical Scaffold for Potent and Sustained Modulation of Gene Expression throughout the Central Nervous System. *Nat. Biotechnol.* **2019**, *37* (8), 884–894. https://doi.org/10.1038/s41587-019-0205-0.

(18) Laina, A.; Gatsiou, A.; Georgiopoulos, G.; Stamatelopoulos, K.; Stellos, K. RNA Therapeutics in Cardiovascular Precision Medicine. *Front. Physiol.* **2018**, *Volume 9-2018*.

(19) Davis, S. M.; Hildebrand, S.; MacMillan, H. J.; Monopoli, K. R.; Buchwald, J.; Sousa, J.; Cooper, D.; Ly, S.; Echeverria, D.; McHugh, N.; Ferguson, C.; Coles, A.; Hariharan, V. N.; O'Reilly, D.; Tang, Q.; Furgal, R.; Yamada, K.; Alterman, J. F.; Gilbert, J. W.; Knox, E.; Pineda, Y.; Weston, C. N.; Baer, C. E.; Pai, A. A.; Khvorova, A. Systematic Analysis of siRNA and mRNA Features Impacting Fully Chemically Modified siRNA Efficacy. *Nucleic Acids Res.* **2025**, *53* (12), gkaf479. https://doi.org/10.1093/nar/gkaf479.

(20) Schwarz, D. S.; Ding, H.; Kennington, L.; Moore, J. T.; Schelter, J.; Burchard, J.; Linsley, P. S.; Aronin, N.; Xu, Z.; Zamore, P. D. Designing siRNA That Distinguish between Genes That Differ by a Single Nucleotide. *PLoS Genet.* **2006**, *2* (9), e140. https://doi.org/10.1371/journal.pgen.0020140.

(21) Hickerson, R. P.; Smith, F. J. D.; Reeves, R. E.; Contag, C. H.; Leake, D.; Leachman, S. A.; Milstone, L. M.; McLean, W. H. I.; Kaspar, R. L. Single-Nucleotide-Specific siRNA Targeting in a Dominant-Negative Skin Model. *J.*

2026 Shanghai School Science Award 仅用于2026上海科学奖论文公示

Invest. Dermatol. **2008**, *128* (3), 594–605. https://doi.org/10.1038/sj.jid.5701060.
(22) Ohnishi, Y.; Tamura, Y.; Yoshida, M.; Tokunaga, K.; Hohjoh, H. Enhancement of Allele Discrimination by Introduction of Nucleotide Mismatches into siRNA in Allele-Specific Gene Silencing by RNAi. *PLoS One* **2008**, *3* (5), e2248. https://doi.org/10.1371/journal.pone.0002248.
(23) Huang, H.; Qiao, R.; Zhao, D.; Zhang, T.; Li, Y.; Yi, F.; Lai, F.; Hong, J.; Ding, X.; Yang, Z.; Zhang, L.; Du, Q.; Liang, Z. Profiling of Mismatch Discrimination in RNAi Enabled Rational Design of Allele-Specific siRNAs. *Nucleic Acids Res.* **2009**, *37* (22), 7560–7569. https://doi.org/10.1093/nar/gkp835.
(24) Liu, J.; Pendergraff, H.; Narayanannair, K. J.; Lackey, J. G.; Kuchimanchi, S.; Rajeev, K. G.; Manoharan, M.; Hu, J.; Corey, D. R. RNA Duplexes with Abasic Substitutions Are Potent and Allele-Selective Inhibitors of Huntingtin and Ataxin-3 Expression. *Nucleic Acids Res.* **2013**, *41* (18), 8788–8801. https://doi.org/10.1093/nar/gkt594.
(25) Tang, Q.; Khvorova, A. RNAi-Based Drug Design: Considerations and Future Directions. *Nat. Rev. Drug Discov.* **2024**, *23* (5), 341–364. https://doi.org/10.1038/s41573-024-00912-9.
(26) Shi, Y.; Zhen, X.; Zhang, Y.; Li, Y.; Koo, S.; Saiding, Q.; Kong, N.; Liu, G.; Chen, W.; Tao, W. Chemically Modified Platforms for Better RNA Therapeutics. *Chem. Rev.* **2024**, *124* (3), 929–1033. https://doi.org/10.1021/acs.chemrev.3c00611.
(27) Wang, S.; Weissman, D.; Dong, Y. RNA Chemistry and Therapeutics. *Nat. Rev. Drug Discov.* **2025**, *24* (11), 828–851. https://doi.org/10.1038/s41573-025-01237-x.
(28) Xu, S.; Xiao, Y.; Li, L.; Yu, L.; Jiang, H.; Yu, A.; Zeng, S. Three New shRNA Expression Vectors Targeting the CYP3A4 Coding Sequence to Inhibit Its Expression. *Acta Pharm. Sin. B* **2014**, *4* (5), 350–357. https://doi.org/10.1016/j.apsb.2014.08.003.

2026 S.-T. Yau High School Science Award
仅用于2026丘成桐中学科学奖公示